T	temperature, K
T_c	critical temperature, K
T_{cm}	critical temperature of mixture, K
V	molar volume, cm^3/mol
V_c	critical molar volume, cm^3/mol
V_{cm}	critical molar volume of mixture, cm^3/mol
x	mole fraction of R 13B1, mol/mol
w	mass fraction of R 13B1, kg/kg
Δ_P	adjustable parameter in eq 2, MPa
Δ_T	adjustable parameter in eq 1, K
Δ_V	adjustable parameter in eq 3, cm^3/mol
θ	surface fraction
ρ	density, kg/m^3
ρ_c	critical density, kg/m^3

Registry No. R 13B1, 75-63-8; R 114, 76-14-2.

Literature Cited

(1) Cooper, W. D.; Borchardt, H. J. *Proc. 15th Int. Congr. Refrig. Int. Inst. Refrig., Venice* **1979**, 995.
(2) Sanyo Electric Trading Co. Ltd. Technical Report, 1983.
(3) Higashi, Y.; Okazaki, S.; Takaishi, Y.; Uematsu, M.; Watanabe, K. *J. Chem. Eng. Data* **1984**, *29*, 31.
(4) Higashi, Y.; Uematsu, M.; Watanabe, K. *Int. J. Thermophys.* **1986**, *7*, 29.
(5) Takaishi, Y.; Kagawa, N.; Uematsu, M.; Watanabe, K. *Proc. 8th Symp. Thermophys. Prop.* **1981**, *2*, 387.
(6) Takaishi, Y.; Uematsu, M.; Watanabe, K. *Bull. JSME* **1982**, *25*, 944.
(7) Takaishi, Y.; Kagawa, N.; Uematsu, M.; Watanabe, K. *Bull. JSME* **1984**, *27*, 1696.
(8) Hasegawa, N.; Uematsu, M.; Watanabe, K. *J. Chem. Eng. Data* **1985**, *30*, 32.
(9) Hosotani, S.; Maezawa, Y.; Uematsu, M.; Watanabe, K. *J. Chem. Eng. Data*, in press.
(10) Okazaki, S.; Higashi, Y.; Takaishi, Y.; Uematsu, M.; Watanabe, K. *Rev. Sci. Instrum.* **1983**, *54*, 21.
(11) Higashi, Y.; Uematsu, M.; Watanabe, K. *Bull. JSME* **1985**, *28*, 2660.
(12) Higashi, Y.; Uematsu, M.; Watanabe, K. *Bull. JSME* **1985**, *28*, 2968.
(13) Higashi, Y.; Ashizawa, M.; Kabata, Y.; Majima, T.; Uematsu, M.; Watanabe, K. *JSME Int. J.* **1987**, *30*, 1106.
(14) Reid, R. C.; Prausnitz, J. M.; Sherwood, T. K. *The Properties of Gases and Liquids*, 3rd ed.; McGraw-Hill: New York, 1977.
(15) Li, C. C. *Can. J. Chem. Eng.* **1971**, *49*, 709.
(16) Chueh, P. L.; Prausnitz, J. M. *AIChE J.* **1967**, *13*, 1107.
(17) Kreglewski, A.; Kay, W. B. *J. Phys. Chem.* **1969**, *73*, 3359.
(18) Soave, G. *Chem. Eng. Sci.* **1972**, *27*, 1197.
(19) Peng, D.; Robinson, D. B. *Ind. Eng. Chem., Fundam.* **1976**, *15*, 59.

Received for review March 16, 1987. Accepted September 16, 1987. We are greatly indebted to the National Research Laboratory of Metrology, Ibaraki, Japan, for the calibration of the thermometer, to Shin-etsu Chemicals Co., Ltd., Tokyo, for kindly furnishing the silicone oil, and also to Du Pont-Mitsui Fluorochemicals Co. Ltd., Tokyo, for kindly furnishing the sample. Financial support of the Grant-in-Aid for Scientific Research Fund in 1985 (Project No. 60790040) by the Ministry of Education, Science and Culture, Japan, to Y.H. is gratefully appreciated.

Vapor–Liquid Equilibria for the Ammonia–Methanol–Water System

Hiroshi Inomata, Noboru Ikawa, Kunio Arai, and Shozaburo Saito*

Department of Chemical Engineering, Tohoku University, Aramaki, Aoba, Sendai, Japan 980

Vapor–liquid equilibrium data are reported for the ammonia–water system at 60 °C and the ammonia–water system at 40 and 60 °C at pressures up to 2.5 MPa. Isobaric vapor–liquid equilibrium data are reported for the ammonia–methanol–water system at 2.0 MPa and at 60, 100, and 140 °C. A new apparatus was developed for these measurements and good agreement with available literature data of Kudo and Toriumi for the ammonia–methanol system could be obtained. Correlation of the data with the Patel–Teja equation of state and van der Waals random mixing rules failed to reproduce the curvature of the *P*–*x* diagrams; however, mixing rules based on Wilson's local composition model could reproduce the detailed system behavior.

Introduction

To recover unreacted ammonia and methanol in the amine production process, it is necessary to separate these components from water. Distillation at atmospheric pressure is currently used for such separation; however, separation at high pressure might be suitable from the viewpoint of energy requirements because the reactor in the amine process is operated at high pressure and, in addition, the latent heat of vaporization at high pressure is smaller compared with that at low pressure.

A knowledge of the vapor–liquid equilibria for the mixtures consisting of ammonia, methanol, and water is essential for the design of such high-pressure separation processes. In this work, the vapor–liquid equilibria for the above-mentioned ternary systems was measured at high pressure and correlated with an equation of state.

Experimental Section

Materials. Methanol with purity 99.6% was obtained from Wako Pure Chemical Industries Ltd., and liquified ammonia was available in relatively high purity (99.97%) from Nippon Sanso Products. No secondary peaks could be detected from gas chromatographic analysis. Water was ion-exchanged and purified through distillation.

Apparatus and Procedure. A schematic diagram of the apparatus developed in this study is shown in Figure 1. This static-type apparatus, in which coexisting phases were continuously circulated, consisted of (1) a dual-windowed equilibrium cell; (2) a recycling system for each coexisting phase; and (3) a sampling and analyzing system. Each part of the apparatus was immersed in a constant temperature air bath controlled to an accuracy of better than ±1 °C. Figure 2 shows the details of the 750 cm^3 internal volume equilibrium cell which was machined from 316 type stainless steel. A methanol–water mixture of known amount and composition was pumped into the evacuated equilibrium cell, 1, by a charging pump, 3. Ammonia was first transferred to the sample cylinder, 12, from the gas cylinder, 14, and then to the cell, 1. The desired pressure was obtained by controlling the vapor pressure of ammonia in the sample cylinder. Equilibrium was achieved by stirring with magnetic stirrer, 8, and recirculating of each phase with the magnetic pumps, 7. To avoid composition change by the condensation of the polar components during recirculation of the vapor phase, the temperature of the recirculation tubing was maintained at slightly higher (2–3 °C) than the equilibrium temperature, whereas the temperature for the liquid phase recirculation tubing was slightly lower (2–3 °C) than the equilibrium temperature to avoid vaporization of the liquid phase. The change of the cell temperature due to this temperature control of the recirculation tubings was determined to be negligible.

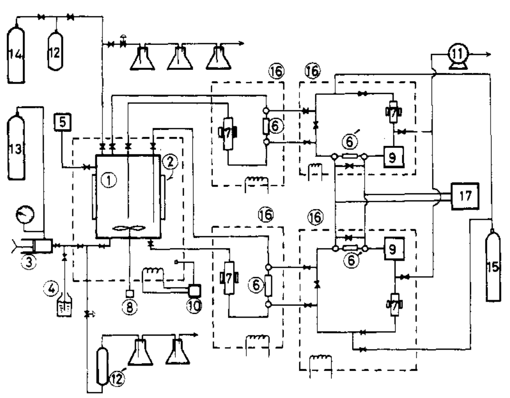

Figure 1. Schematic diagram of experimental apparatus: (1) equilibrium cell; (2) window; (3) sample charging pump; (4) liquid sample; (5) pressure transducer; (6) sampler; (7) magnetic pump; (8) magnetic stirrer; (9) flash tank; (10) temperature controller; (11) vacuum pump; (12) NH_3 sample cylinder; (13) N_2 gas cylinder; (14) NH_3 gas cylinder; (15) He gas cylinder; (16) air bath; (17) gas chromatograph.

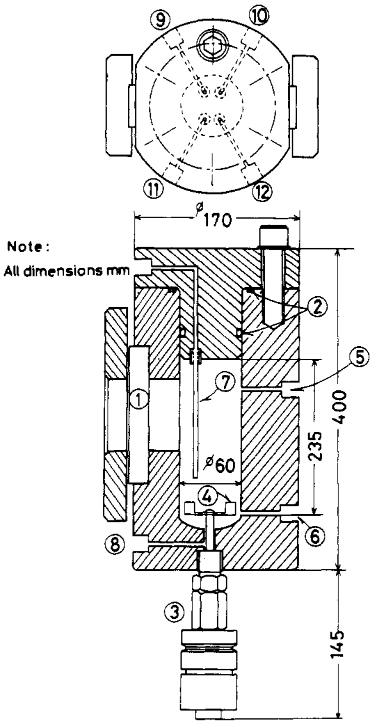

Figure 2. Equilibrium cell: (1) borosilicate glass window; (2) silicone O-ring; (3) magnetic stirrer; (4) impeller; (5) thermowell; (6) liquid-phase outlet; (7) vapor or liquid inlet or outlet arrangement; (8) sample feed inlet; (9) liquid-phase inlet; (10) pressure tap; (11) vapor-phase inlet; (12) vapor-phase outlet.

Table I. Vapor-Liquid Equilibrium Data for the NH_3 (1)-CH_3OH (2) System

		vapor phase		liquid phase	
press., MPa	temp, °C	NH_3	CH_3OH	NH_3	CH_3OH
		40 °C			
0.12	39.9	0.745	0.255	0.201	0.799
0.32	40.0	0.941	0.059	0.382	0.618
0.55	40.0	0.976	0.024	0.510	0.490
0.74	39.9	0.986	0.014	0.604	0.396
0.89	39.5	0.990	0.010	0.681	0.319
0.99	39.8	0.992	0.008	0.713	0.287
1.19	39.8	0.996	0.004	0.809	0.191
1.37	39.9	0.998	0.002	0.893	0.107
		60 °C			
0.22	58.9	0.632	0.368	0.166	0.834
0.55	58.9	0.901	0.099	0.368	0.632
1.18	59.5	0.969	0.031	0.572	0.428
1.65	59.1	0.985	0.015	0.705	0.295
2.00	59.1	0.992	0.008	0.798	0.202
2.44	60.1	0.998	0.002	0.936	0.064

Table II. Vapor-Liquid Equilibrium Data for the NH_3 (1)-Water (2) System (at 60 °C)

		vapor phase		liquid phase	
press., MPa	temp, °C	NH_3	H_2O	NH_3	H_2O
0.16	59.6	0.928	0.072	0.197	0.804
0.34	59.8	0.975	0.025	0.318	0.682
0.65	59.8	0.991	0.009	0.440	0.560
1.06	59.6	0.996	0.004	0.554	0.446
1.55	59.7	0.998	0.002	0.683	0.317
2.07	59.8	0.999	0.001	0.832	0.168

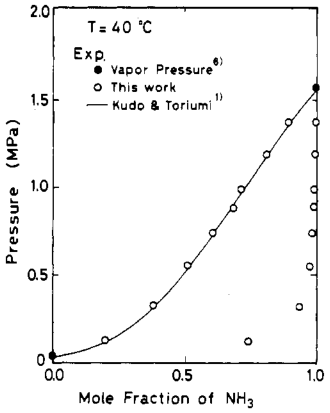

Figure 3. Comparison between the experimental and literature data for the ammonia-methanol system at 40 °C.

When the stirring and the circulation were stopped, a small amount of each phase was isolated in the sampler, 6, expanded into an evacuated tank, 9, and recirculated with magnetic pump to homogenize the composition throughout the sampling system.

The equilibrium compositions were determined by analyzing the sample in the sampler 6′ of the analyzing system by a gas chromatograph (Hitachi GC-163) equipped with a thermal conductivity detector (TCD). The chromatographic peaks were measured with a commercial electronic integrator (Shimadzu C-R1B). The current of the TCD was 100 mA. A glass column (3 m long × 3 mm i.d.), packed with PEG6000 (10%) + KOH (1%)/Chromosorb-103, was used and operated isothermally at 80 °C. Helium carrier gas was used at a flow rate of 37.5 cm^3/min. Mole fractions were determined by using the calibration curves obtained from analyses of gravimetrically prepared samples. The accuracy of the calibration curves was estimated to be better than ±2.5%. Each sample was analyzed at least three times and the reproducibility was within 1%. The overall uncertainty in the equilibrium compositions is estimated to be ±0.5 mol %.

The equilibrium temperature was measured with a chromel-alumel thermocouple inserted into the equilibrium cell, whose calibration was made against the two fixed points of the ITPS-68. The accuracy of this calibration is better than 0.1 °C for 0-200 °C range. The equilibrium pressure was measured with a pressure transducer whose accuracy was checked by a dead weight tester to be 0.01 MPa.

Experimental Results. Vapor-liquid equilibria were measured for the binary system of ammonia-water at 60 °C and ammonia-methanol at 40 and 60 °C. In addition, isobaric vapor-liquid equilibrium measurements were made for the ammonia-methanol-water system at 60, 100, and 140 °C. These raw data are presented in Tables I-III.

To test the reliability of the experimental results, measurement data for the ammonia-methanol system were compared with the smoothed solubility data of Kudo and Toriumi (*1*) shown in Figure 3. Agreement is good within 0.01 in liquid-phase mole

Table III. Vapor–Liquid Equilibria for the NH_3 (1)–CH_3OH (2)–H_2O (3) System

		vapor phase			liquid phase		
temp, °C	press., MPa	NH_3	CH_3OH	H_2O	NH_3	CH_3OH	H_2O
			60 °C, 2.0 MPa				
60.0	2.02	0.993	0.006_7	0.000_5	0.809	0.184	0.007
60.6	2.07	0.995	0.004_7	0.000_7	0.838	0.130	0.032
60.0	2.06	0.996	0.003_4	0.000_6	0.852	0.080	0.068
59.8	2.04	0.997	0.002_5	0.000_8	0.853	0.058	0.089
60.1	2.05	0.998	0.001_4	0.000_9	0.849	0.034	0.117
59.9	2.02	0.998	0.000_5	0.001_2	0.839	0.012	0.149
59.2	1.99	0.992	0.008_0		0.798	0.202	
59.8	2.07	0.999		0.001	0.832		0.168
			100 °C, 2.0 MPa				
99.7	2.03	0.955	0.032	0.013	0.504	0.141	0.355
99.2	2.07	0.952	0.033	0.015	0.508	0.158	0.334
99.8	2.07	0.938	0.052	0.010	0.498	0.245	0.257
100.6	2.04	0.917	0.077	0.006	0.486	0.380	0.134
99.9	2.01	0.877	0.123		0.458	0.542	
100.0	2.03	0.975		0.025	0.478		0.522
			140 °C, 2.0 mPa				
141.4	1.99	0.708	0.236	0.056	0.265	0.282	0.453
141.1	2.03	0.767	0.167	0.066	0.276	0.200	0.524
141.0	2.04	0.647	0.306	0.047	0.257	0.432	0.311
140.9	2.05	0.604	0.356	0.040	0.236	0.508	0.256
141.4	2.05	0.857	0.003	0.140	0.269	0.003	0.728
138.3	2.07	0.544	0.456		0.220	0.780	

fraction and 0.02 MPa in bubble pressure.

Correlation

The experimental *TPXY* data in Tables I–III were correlated with the Patel–Teja cubic equation of state because it has been shown to be more accurate than other similar equations. It has the form (*2*)

$$P = RT/(v - b) - a/[v(v + b) + c(v - b)] \tag{1}$$

The generalized expressions for the equation of state parameters a, b, and c were used in this study since it was found that they gave similar results to the substance-dependent parameters proposed by Patel and Teja for the present systems.

For mixtures, the random mixing rules suggested by ref *2* failed to represent the P–x diagram curvature. Present methods do not give adequate correlation of the highly polar system. Therefore we applied a two-fluid mixing rule based on Wilson's local composition model (*3*) expressed as follows (*4*)

$$a_m = \sum_i x_i \sum_j x_{ji}(a_j a_i)^{0.5} \tag{2}$$

$$x_{ji} = x_j \eta_{ji} / (\sum_k x_k \eta_{ki}) \tag{3}$$

$$\eta_{ji} = \exp[-(\lambda_{ji} - \lambda_{ii})/RT] \tag{4}$$

$$b_m = \sum_i x_i b_i \tag{5}$$

$$c_m = \sum_i x_i c_i \tag{6}$$

where x_{ji} is the local mole fraction of molecule j around molecule i, and λ_{ji} is the interaction energy between molecules j and i and is equal to λ_{ij}.

The values of the energy parameters η_{ij} ($\neq \eta_{ji}$) were determined by minimizing the least-squares error along with the experimental temperature and pressure in predicted equilibrium compositions of the binary systems given as

$$E = \frac{1}{N} \sum_i^N \{(x_i^{\text{calcd}} - x_i^{\text{exptl}})^2 + (y_i^{\text{calcd}} - y_i^{\text{exptl}})^2\} \tag{7}$$

where N is the number of data. For the methanol–water system, the data of Bredig and Bayer (*5*) were used to determine optimum η_{ij} values. Figure 4 shows the comparison for the ternary system of ammonia–methanol–water between the experimental data and the prediction results with Patel–Teja equation of state and the optimum η_{ij}. Agreement between the predicted and experimental tie lines is fairly good although the calculated conjugate lines are not yet satisfactory.

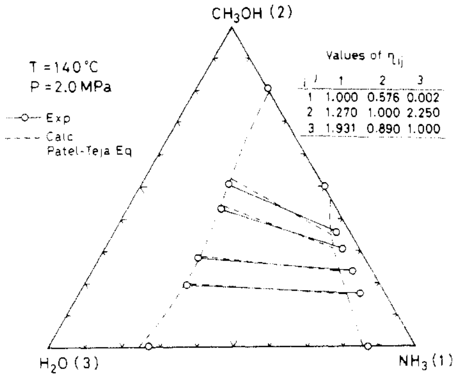

Figure 4. Experimental and calculated vapor–liquid equilibria for the ammonia–methanol–water system.

Conclusion

Vapor–liquid equilibrium measurements were made for the binary systems of ammonia–methanol and ammonia–water, and for the ammonia–methanol–water ternary system. These data should be useful in engineering design and developing new mixing rules for polar mixtures. Measurement data for the ternary system could be correlated with the Patel–Teja equation of state and a local composition mixing rule.

Glossary

a, b, c	parameters of Patel–Teja equation of state
P	pressure, Pa
R	universal gas constant, J mol^{-1} K^{-1}
T	temperature, K
v	molar volume, m^3 mol^{-1}
x_i	mole fraction of molecule i
x_{ji}	local mole fraction of molecule j around molecule i

Greek Letters

λ_{ji}	interaction energy between molecules j and i
η_{ji}	energy parameter between molecules j and i

Superscripts

calcd	calculated value
exptl	experimental value

Registry No. NH_3, 7664-41-7; MeOH, 67-56-1.

Literature Cited

(1) Kudo, S.; Toriumi, T. *Bull. Chem. Res. Inst. Non-Aqueous Solution Tohoku Univ.* **1959**, *8*, 27.
(2) Patel, N. C.; Teja, A. C. *Chem. Eng. Sci.* **1982**, *37*, 463.
(3) Wilson, G. M. *J. Am. Chem. Soc.* **1964**, *86*, 127.
(4) Takishima, S.; Saiki, K.; Arai, K.; Saito, S. *J. Chem. Eng. Jpn.* **1986**, *19*, 48.
(5) Bredig, G.; Bayer, R. *Z. Phys. Chem.* **1927**, *130*, 1.
(6) Vargaftik, N. B. *Tables on The Thermophysical Properties of Liquids and Gases*, 2nd ed.; Hemisphere: Washington, DC, 1975.

Received for review September 29, 1986. Revised manuscript received May 6, 1987. Accepted August 12, 1987.

Solubility and Diffusivity of Acid Gases (CO_2, N_2O) in Aqueous Alkanolamine Solutions

Geert F. Versteeg* and Wim P. M. van Swaaij

Department of Chemical Engineering, Twente University of Technology, 7500 AE Enschede, The Netherlands

Solubility and diffusivity of N_2O and CO_2 in water were determined as a function of temperature from the results published in the open literature, and new data were measured in the present work. The solubility of N_2O in several aqueous alkanolamine (DEA, DIPA, DMMEA, and DIPA) solutions at various temperatures was measured and correlated over a wide range of conditions. For both the diffusivity of N_2O and the alkanolamine in aqueous alkanolamine solutions a modified Stokes–Einstein relation was derived. With the aid also of the "N_2O analogy" the diffusivity of CO_2 in these solutions can be estimated.

1. Introduction

Alkanolamines have become one of the most important classes of chemicals for the removal of the acid gas components H_2S and CO_2 from several types of gases. Frequently, aqueous solutions are applied; however, mixtures of water and a nonaqueous solvent are also used (e.g., Shell-Sulfinol process (*1*)). Diisopropanolamine (DIPA), methyldiethanolamine (MDEA), monoethanolamine (MEA), and diethanolamine (DEA) are examples of well-known and industrially important amines (Kohl and Riesenfeld (*1*)).

For the design of suitable gas–liquid contactors for the above-mentioned gas-treating processes it is necessary that the mass-transfer rates can be calculated accurately. Besides needed information on the mass-transfer coefficients, gas–liquid contact area, and reaction kinetics, data are also needed on the fundamental physicochemical properties like the solubility and the diffusivity of the acid gas components in the various solutions. However, due to the chemical reaction that occurs in the solution, it is not possible to obtain information directly on these properties and therefore they must be estimated from corresponding data of more or less similar nonreacting gases.

In view of the similarities with regard to configuration, molecular volume, and electronic structure, N_2O is often used as nonreacting gas to estimate the properties of CO_2. Laddha et al. (*2*) investigated the solubility of N_2O and CO_2 in aqueous solutions of organic compounds that are nonreacting with respect to both solutes and organic alcohols that have a somewhat similar structure to MEA and DEA. From this work it was concluded that the ratio of the solubilities remained constant for the various solutions and that the "N_2O analogy" may be applied to estimate the solubility of CO_2 in aqueous alkanolamine solutions according to the equation

$$(\text{solubility of } CO_2) = C_1(\text{solubility of } N_2O) \tag{1}$$

with

$$C_1 = (\text{solubility of } CO_2 \text{ in water})/(\text{solubility of } N_2O \text{ in water}) \tag{2}$$

Sada et al. (*3*, *4*) mentioned earlier that the N_2O analogy could be used to obtain information on the solubility of CO_2 and also considered that a relation similar to eq 1 could be applied to estimate the diffusivity of CO_2. From Sada et al.'s (*3*, *4*) results, however, it was not possible to derive a general correlation to calculate the diffusivity of N_2O (or CO_2) in aqueous alkanolamine solutions. Versteeg (*5*) recently published additional data on the diffusivity of N_2O in aqueous alkanolamine solutions, and these data showed a good agreement with the results of Sada et al. (*4*) although for DEA a substantial deviation occurred. Nevertheless, it may be possible to obtain a general (e.g., a modified Stokes-Einstein relation) relation that is able to calculate the diffusivity.

Haimour and Sandall (*6*) studied the absorption of CO_2 and N_2O in aqueous MDEA solutions at various temperatures in a laminar liquid jet. At very short contact times the absorption of CO_2 can be considered as physical absorption without any enhancement due to the chemical reaction and therefore it was possible to verify for this particular solution the N_2O analogy for both solubility and diffusivity combined in the physicochemical parameter $mD^{1/2}$. From their results it could be concluded that for aqueous MDEA solutions the "analogy" holds.

In the present work new data on both solubility and diffusivity of N_2O in aqueous alkanolamine solutions at various temperatures will be presented and for CO_2, using the N_2O analogy, both properties can be estimated. The available data of the solubility and diffusivity of CO_2 and N_2O in water published in the open literature are summarized in combination with these new data.

2. Solubility

2.1. ***Experimental Procedure.*** The solubility was measured in a glass vessel with a volume of 1.05×10^{-3} m^3 which was filled with a calibrated volume (4.02×10^{-4} m^3) of solution. In each experiment the solution was degassed by means of evacuation of the equilibrium vessel and the contents were held under vacuum until bubbles of air ceased to be evolved by the liquid and then the vapor–liquid equilibrium was established. Equilibrium pressure was recorded by a pressure transducer. The appropriate gas was then fed to the vessel until a arbitrary

0021-9568/88/1733-0029$01.50/0